assistance from E. MacLennan and D. Luscombe in performing some of the electrochemical experiments is also gratefully acknowledged.

Registry No. 1, 98395-25-6; **4a**, 69881-14-7; **4b**, 63950-13-0; $(\eta\text{-}C_5H_5)_2Rh_2(CO)(CNEt)(\mu\text{-}CF_3C_2CF_3)$, 110294-86-5; $(\eta\text{-}C_5H_5)_2Rh_2(CO)(CN\text{-}i\text{-}Pr)(\mu\text{-}CF_3C_2CF_3)$, 98464-05-2; $(\eta\text{-}C_5H_5)_2Rh_2(CO)(CNCy)(\mu\text{-}CF_3C_2CF_3)$, 98464-04-1; $(\eta\text{-}C_5H_5)_2Rh_2(CO)(CNC_6H_3Me_2)(\mu\text{-}CF_3C_2CF_3$, 110294-85-4; $p\text{-}MeC_6H_4NCO$, 622-58-2; $(\eta\text{-}C_5H_5)_3Rh_3(\mu\text{-}CO)(\mu\text{-}CF_3C_2CF_3)$, 37343-45-6; $(\eta\text{-}C_5H_5)_2Rh_2\{\mu\text{-}\eta^3\text{-}N(C_6H_4Me\text{-}p)C(O)C(CF_3)C(CF_3)\}$, 90883-05-9; $(\eta\text{-}C_5H_5)_3Rh_3\{\mu\text{-}C(CF_3)\}_2$, 110294-87-6; $(\eta\text{-}C_5H_5)_2Rh_2\{C_4(CF_3)_4\}$, 39385-05-2; $(\eta\text{-}C_5H_5)_2Rh_2\{\mu\text{-}\eta^3\text{-}N(Me)C(O)C(CF_3)C(CF_3)\}$, 90860-65-4; $(\eta\text{-}C_5H_5)_2Rh_2\{\mu\text{-}\eta^3\text{-}N(t\text{-}Bu)C(O)C(CF_3)C(CF_3)\}$, 90860-66-5; $(\eta\text{-}C_5H_5)_2Rh_2(CO)(CNC_6H_4OMe\text{-}p)(\mu\text{-}CF_3C_2CF_3)$, 110294-84-3; $(\eta\text{-}C_5H_5)_2Rh_2\{\mu\text{-}\eta^3\text{-}N(C_6H_4OMe\text{-}p)C(O)C(CF_3)C(CF_3)\}$, 110294-88-7; $(\eta\text{-}C_5H_5)_2Rh_2\{\mu\text{-}\eta^3\text{-}N(C_2H_5)C(O)C(CF_3)C(CF_3)\}$, 110294-89-8; $(\eta\text{-}C_5H_5)_2Rh_2\{\mu\text{-}\eta^3\text{-}N(C_6H_3Me_2\text{-}2,6)C(O)C(CF_3)C(CF_3)\}$, 110294-90-1; $(\eta\text{-}C_5H_5)_2Rh_2\{\mu\text{-}\eta\text{-}N(C_6H_4NO_2\text{-}p)C(O)C(CF_3)C(CF_3)\}$, 110294-91-2; $(\eta\text{-}C_5H_5)_2Rh_2(CO)(CNC_6H_4NO_2\text{-}p)(\mu\text{-}CF_3C_2CF_3)$, 110294-83-2; C_2H_5NCO, 624-79-3; $i\text{-}PrNCO$, 598-45-8; CyNCO, 931-53-3; $2,6\text{-}Me_2C_6H_4NCO$, 2769-71-3; MeNCO, 624-83-9; $t\text{-}BuNCO$, 1609-86-5; $(\eta\text{-}C_5H_5)_2Rh_2(CO)(CN\text{-}t\text{-}Bu)(\mu\text{-}CF_3C_2CF_3)$, 71853-17-3; $(\eta\text{-}C_5H_5)_2Rh_2(CO)(PPh_3)(\mu\text{-}CF_3C_2CF_3)$, 110351-10-5.

Supplementary Material Available: Tables of thermal parameters, ligand geometries, and equations for planes for $(\eta\text{-}C_5H_5)_2Rh_2(CO)(CNC_6H_3Me_2\text{-}2,6)(CF_3C_2CF_3)$ (4 pages); a listing of structure factor amplitudes (13 pages). Ordering information is given on any current masthead page.

Addition of Small Molecules to $(\eta\text{-}C_5H_5)_2Rh_2(CO)(CF_3C_2CF_3)$. 8.[1] Solution Behavior of the Isocyanide Complexes $(\eta\text{-}C_5H_5)_2Rh_2(CO)(CNR)(CF_3C_2CF_3)$ and Their Conversion to $(\eta\text{-}C_5H_5)_2Rh_2(CO)\{C(NR)C(CF_3)C(CF_3)\}$. Crystal and Molecular Structure of $(\eta\text{-}C_5H_5)_2Rh_2(CO)\{C(NEt)C(CF_3)C(CF_3)\}$

Ron S. Dickson,* Gary D. Fallon, Rhonda J. Nesbit, and Helen Pateras

Department of Chemistry, Monash University, Clayton, Victoria 3168, Australia

Received March 25, 1987

Coordinative addition of isocyanides CNR to $(\eta\text{-}C_5H_5)_2Rh_2(\mu\text{-}CO)(\mu\text{-}CF_3C_2CF_3)$ gives $(\eta\text{-}C_5H_5)_2Rh_2(CO)(CNR)(\mu\text{-}CF_3C_2CF_3)$ (1) which isomerizes in solution when R = Et, *i*-Pr, Cy, Ph, $p\text{-}MeOC_6H_4$, or $p\text{-}NO_2C_6H_4$ to **2**. Spectroscopic analysis establishes that **2** can be formulated as $(\eta\text{-}C_5H_5)_2Rh_2(CO)\{\mu\text{-}C(NR)C(CF_3)C(CF_3)\}$ and that it exists as a mixture of three interconverting isomers **2a**, **2b**, and **2c** in solution. The rate of interconversion between the various isomers has been investigated by variable-temperature NMR and varies according to R, being greatest for the aryl systems. The isomer distribution **2a**:**2b**:**2c** is both solvent- and temperature-dependent. The molecular structure of **2a**, R = Et, has been determined by X-ray crystallography. Crystal data: $C_{18}H_{15}F_6NORh_2$, M_r 581.2, monoclinic, $P2_1/n$, a = 14.636 (8) Å, b = 11.277 (6) Å, c = 11.774 (6) Å, β = 92.86 (9)°, Z = 4, final R = 0.056 for 2771 "observed" reflections. A bridging allylimine ligand and a terminal carbonyl are indicated for this isomer in the solid state. The reaction kinetics for the isomerization of **1** to **2** have been determined from NMR data. The rate of isomerization depends markedly on R and follows the sequence R = Cy ($t_{1/2}$ = 1740 min) < *i*-Pr < Ph < $p\text{-}MeOC_6H_4$ < $p\text{-}NO_2C_6H_4$ ($t_{1/2}$ = 1.4 min). The interconversion rates between isomers of **2** follow the same sequence.

Introduction

We have shown previously that the coordinative addition of ligands to $(\eta\text{-}C_5H_5)_2Rh_2(\mu\text{-}CO)(\mu\text{-}CF_3C_2CF_3)$ is frequently followed by facile intramolecular reactions between the added ligand and the coordinated hexafluorobutyne. The formation of bridging pentadienones,[2,3] bridging acrylamides,[4] and bridging allyl groups[5] when alkynes, isocyanates, and carbenes, respectively, are added provides examples of this type of behavior. As indicated in a previous paper,[1] the addition of isocyanides, CNR, to $(\eta\text{-}C_5H_5)_2Rh_2(\mu\text{-}CO)(\mu\text{-}CF_3C_2CF_3)$ results in the formation of $(\eta\text{-}C_5H_5)_2Rh_2(CO)(CNR)(\mu\text{-}CF_3C_2CF_3)$ which in many instances rapidly convert to isomeric species. In this paper, we unravel the nature of these isomeric species, and we describe the solution behavior of the systems.

Experimental Section

The general procedures and instrumentation used are described in the previous paper.[1] Literature procedures[6] were followed in preparing the following isocyanide ligands: PhNC, $p\text{-}MeOC_6H_4NC$, $p\text{-}NO_2C_6H_4NC$.

Formation of $(\eta\text{-}C_5H_5)_2Rh_2(CO)\{\mu\text{-}C(NR)C(CF_3)C(CF_3)\}$. The preparation of $(\eta\text{-}C_5H_5)_2Rh_2(CO)(CNR)(\mu\text{-}CF_3C_2CF_3)$ from $(\eta\text{-}C_5H_5)_2Rh_2(\mu\text{-}CO)(\mu\text{-}CF_3C_2CF_3)$ and CNR in dichloromethane at 20 °C has been described previously.[1] When left in solution (CH_2Cl_2, 20 °C), these complexes undergo structural rearrangements to give new species $(\eta\text{-}C_5H_5)_2Rh_2(CO)\{\mu\text{-}C(NR)C(CF_3)C(CF_3)\}$. The combined yield of $(\eta\text{-}C_5H_5)_2Rh_2(CO)(CNR)(\mu\text{-}CF_3C_2CF_3)$ and $(\eta\text{-}C_5H_5)_2Rh_2(CO)\{\mu\text{-}C(NR)C(CF_3)C(CF_3)\}$ is generally between 90 and 100%, and the proportion of the two isomers depends upon the age of the solution. The two complexes were separated by TLC (20 × 20 cm plates, 1:1 silica gel G–HF_{254} mixture as adsorbent, plates dried at room temperature only),

(1) Part 7: Bixler, J. W.; Bond, A. M.; Dickson, R. S.; Fallon, G. D.; Nesbit, R. J.; Pateras, H. *Organometallics*, preceding paper in this issue.
(2) Baimbridge, C. W.; Dickson, R. S.; Fallon, G. D.; Grayson, I.; Nesbit, R. J.; Weigold, J. *Aust. J. Chem.* **1986**, *39*, 1187.
(3) Dickson, R. S.; Fallon, G. D.; McLure, F. I.; Nesbit, R. J. *Organometallics* **1987**, *6*, 215.
(4) Dickson, R. S.; Nesbit, R. J.; Pateras, H.; Baimbridge, W.; Patrick, J. M.; White, A. H. *Organometallics* **1985**, *4*, 2128.
(5) Dickson, R. S.; Fallon, G. D.; Nesbit, R. J.; Pain, G. N. *Organometallics* **1985**, *4*, 355.
(6) Shingaki, T.; Takebayashi, M. *Bull. Chem. Soc. Jpn.* **1963**, *36*, 617.

0276-7333/87/2306-2517$01.50/0 © 1987 American Chemical Society

and crystalline solids were obtained by extraction of the bands with CH_2Cl_2 and removal of solvent. Data used to characterize the new complexes are detailed below.

$(\eta$-$C_5H_5)_2Rh_2(CO)\{\mu$-$C(NEt)C(CF_3)C(CF_3)\}$: orange-red crystals; mp 135 °C. Anal. Calcd for $C_{18}H_{15}F_6NORh_2$: C, 37.2; H, 2.6; F, 19.6; N, 2.4. Found: C, 37.1; H, 2.6; F, 19.5; N, 2.5. Spectroscopic data: IR (CH_2Cl_2) ν(CO) at 2000 vs and 1850 m, ν(C=N) at 1750 s and 1680 m cm^{-1}; ^1H NMR ($CDCl_3$) δ 5.62 (m, 10 H × 0.17, C_5H_5'), 5.59 (d, 5 H, J = 0.9 Hz, C_5H_5), 5.55 (s, 5 H × 0.04, C_5H_5''), 5.51 (s, 5 H × 0.04, C_5H_5''), 5.31 (s, 5 H, C_5H_5), 3.6–3.4 (m, 2 H, CH_2), 1.30 (t, 3 H, J = 7 Hz, CH_3); ^{19}F NMR ($CDCl_3$) δ 52.0 (q, 3 F × 0.04, J = 12 Hz, CF_3''), 52.3 (q, 3 F, J = 12 Hz, CF_3), 52.6 (m, 3 F × 0.09, CF_3'), 54.7 (q, 3 F × 0.04, J = 12 Hz, CF_3''), 55.8 (q, 3 F, J = 12 Hz, CF_3), 60.2 (m, 3 F × 0.09, CF_3'); MS, m/z (relative intensity) 581 $[M]^+$ (2), 553 $[M - CO]^+$ (13), 526 $[M - CNEt]^+$ (3), 233 $[C_{10}H_{10}Rh]^+$ (100). [In these and subsequent spectra, there is evidence for one major and two minor isomers in solution. The proportions of the minor isomers are indicated by giving the relative intensities as a mole fraction of those for the major isomer; e.g., (5 H × 0.10) indicates the intensity is 1/10th that of the corresponding peak for the major isomer.]

$(\eta$-$C_5H_5)_2Rh_2(CO)\{\mu$-$C(N$-i-$Pr)C(CF_3)C(CF_3)\}$: orange-red crystals; mp 104–105 °C. Anal. Calcd for $C_{19}H_{17}F_6NORh_2$: C, 38.3; H, 2.9; F, 19.2; N, 2.4. Found: C, 38.3; H, 2.7; F, 19.3; N, 2.4. Spectroscopic data: IR (CH_2Cl_2) ν(CO) at 2000 vs and 1845 s, ν(C=N) at 1715 s and 1685 sh cm^{-1}; ^1H NMR ($CDCl_3$) δ 5.61 (br s, 10 H × 0.16, 2 × C_5H_5'), 5.58 (s, 5 H, C_5H_5), 5.55 (s, 5 H × 0.08, C_5H_5''), 5.51 (s, 5 H × 0.08, C_5H_5''), 5.29 (s, 5 H, C_5H_5), 3.25 (sept, 1 H, J = 6 Hz, C*H*), 1.33 and 1.29 (2 × d, 6 H, J = 6 Hz, 2 × CH_3); ^{19}F NMR ($CDCl_3$) δ 51.9 (q, 3 F × 0.08, J = 12 Hz, CF_3''), 52.1 (qd, 3 F, J = 12 and 3 Hz, CF_3), 52.6 (m, 3 F × 0.08, CF_3'), 54.8 (q, 3 F × 0.08, J = 12 Hz, CF_3''), 55.8 (q, 3 F, J = 12 Hz, CF_3), 60.1 (m, 3 F × 0.08, CF_3'); ^{13}C NMR ($CDCl_3$, $Cr(acac)_3$ added as relaxation reagent) δ 191.0 (d, J = 82 Hz, CO), 188.6 (dd, J = 82 and 4 Hz, CO), 89.9 (d, J = 4 Hz, C_5H_5), 87.2 (d, J = 4 Hz, C_5H_5), 60.9 (s, *C*HMe_2), 24.1 and 23.8 (2 × s, CH*Me*$_2$); MS, m/z (relative intensity) 595 $[M]^+$ (12), 583 $[M - C]^+$ (4), 567 $[M - CO]^+$ (12), 233 $[C_{10}H_{10}Rh]^+$ (100).

$(\eta$-$C_5H_5)_2Rh_2(CO)\{\mu$-$C(NCy)C(CF_3)C(CF_3)\}$: orange-red crystals; mp 105–106 °C. Anal. Calcd for $C_{23}H_{21}F_6NORh_2$: C, 41.6; H, 3.3; F, 18.0; N, 2.2. Found: C, 41.5; H, 3.0; F, 18.0; N, 2.2. Spectroscopic data: IR (CH_2Cl_2) ν(CO) at 2010 vs and 1850 m, ν(C=N) at 1730 s, 1690 sh, and 1680 m cm^{-1}; ^1H NMR ($CDCl_3$) δ 5.60 (br s, 10 H × 0.09, 2 × C_5H_5'), 5.56 (s, 5 H, C_5H_5), 5.53 (s, 5 H × 0.09, C_5H_5''), 5.51 (s, 5 H × 0.09, C_5H_5''), 5.28 (s, 5 H, C_5H_5), 2.9 and 2.0–1.1 (br m, 11 H, Cy); ^{19}F NMR ($CDCl_3$) δ 51.8 (q, 3 F × 0.09, J = 12 Hz, CF_3''), 52.2 (qd, 3 F, J = 11 and 4 Hz, CF_3), 52.6 (m, 3 F × 0.09, CF_3'), 54.8 (q, 3 F × 0.09, J = 12 Hz, CF_3''), 55.7 (q, 3 F, J = 11 Hz, CF_3), 60.1 (m, 3 F × 0.09, CF_3'); MS, m/z (relative intensity) 635 $[M]^+$ (7), 607 $[M - CO]^+$ (10), 233 $[C_{10}H_{10}Rh]^+$ (100).

$(\eta$-$C_5H_5)_2Rh_2(CO)\{\mu$-$C(NPh)C(CF_3)C(CF_3)\}$ was the major product obtained from the reaction of phenyl isocyanide with $(\eta$-$C_5H_5)_2Rh_2(CO)(CF_3C_2CF_3)$. It was isolated as orange-brown crystals (60% yield after immediate workup), mp 170 °C. Anal. Calcd for $C_{22}H_{15}F_6NORh_2$: C, 42.0; H, 2.4; F, 18.1; N, 2.2. Found: C, 42.4; H, 2.3; F, 18.1; N, 2.2. Spectroscopic data: IR (CH_2Cl_2) ν(CO) at 2000 vs and 1850 s, ν(C=N) at 1680 sh and 1675 vs cm^{-1}; ^1H NMR ($CDCl_3$) δ 7.6–7.1 (m, 8 H, C_6H_4), 6.7 (m, 2 H, C$_6$H), 5.60 (br, 5 H × 0.89, C_5H_5'), 5.59 (s, 5 H × 0.06, C_5H_5''), 5.55 (br, 5 H, C_5H_5), 5.33 (d, 5 H × 0.06, J = 0.9 Hz, C_5H_5''), 5.32 (br, 5 H, C_5H_5), 5.10 (br, 5 H × 0.89, C_5H_5'); ^{19}F NMR ($CDCl_3$) δ 52.1 (q, 3 F × 0.06, CF_3''), 52.7 (m, 3 F × 1.89, CF_3 + CF_3'), 55.0 (q, 3 F × 0.06, CF_3''), 55.7 (br, 3 F, CF_3), 60.1 (br, 3 F × 0.89, CF_3'); MS, m/z (relative intensity) 629 $[M]^+$ (<5), 601 $[M - CO]^+$ (15), 233 $[C_{10}H_{10}Rh]^+$ (100).

A minor product was isolated as an orange solid and was spectroscopically identified as $(\eta$-$C_5H_5)_2Rh_2(CO)(CNPh)(\mu$-$CF_3C_2CF_3)$ (8% yield after immediate workup). Spectroscopic data: IR (CH_2Cl_2) ν(CN) at 2120 vs, ν(CO) at 1990 s cm^{-1}; ^1H NMR ($CDCl_3$) δ 7.5–7.2 (m, 5 H, C_6H_5), 5.47 (s, 10 H, 2 × C_5H_5); ^{19}F NMR ($CDCl_3$) δ 54.9 (s, CF_3). There was rapid conversion to $(\eta$-$C_5H_5)_2Rh_2(CO)\{\mu$-$C(NPh)C(CF_3)C(CF_3)\}$ when this compound was dissolved in dichloromethane or acetone.

$(\eta$-$C_5H_5)_2Rh_2(CO)\{\mu$-$C(NC_6H_4OMe$-$p)C(CF_3)C(CF_3)\}$ was obtained as the major product when *p*-methoxyphenyl isocyanide was added to $(\eta$-$C_5H_5)_2Rh_2(\mu$-$CO)(\mu$-$CF_3C_2CF_3)$. It was recrystallized from hexane/diethyl ether to give orange-red crystals (64% yield), mp 175 °C. Anal. Calcd for $C_{23}H_{17}F_6NO_2Rh_2$: C, 41.9; H, 2.6; F, 17.3; N, 2.1. Found: C, 42.1; H, 2.6; F, 16.9; N, 2.0. Spectroscopic data: IR (CH_2Cl_2) ν(CO) at 2005 vs and 1850 s, ν(C=N) at 1690 s and 1660 s cm^{-1}, ^1H NMR ($CDCl_3$) δ 7.6–6.9 (m, 4 H, C_6H_4), 5.51 (s, 5 H, C_5H_5), 5.29 (s, 5 H, C_5H_5), 3.85 (s, 3 H, CH_3); ^{19}F NMR ($CDCl_3$) δ 52.0 (q, 3 F × 0.04, CF_3''), 52.7 (q, 3 F × 1.29, J = 12 Hz, CF_3 + CF_3'), 54.9 (q, 3 F × 0.04, CF_3''), 55.6 (br, 3 F, CF_3), 60.1 (br, 3 F × 0.29, CF_3'); ^{13}C NMR ($CDCl_3$, $Cr(acac)_3$) δ 211.2 (m, CO), 188.8 (br d, J = 65 Hz, CO), 188.4 (d, J = 86 Hz, CO), 122.7 (m, C_6H_4), 113.8 (s, C_6H_4), 90.5 (m, C_5H_5), 88.8 (m, C_5H_5), 55.5 (s, OCH_3); MS, m/z (relative intensity) 659 $[M]^+$ (10), 631 $[M - CO]^+$ (18), 233 $[C_{10}H_{10}Rh]^+$ (100).

A minor compound obtained in this reaction is probably $(\eta$-$C_5H_5)_2Rh_2(CO)(CNC_6H_4OMe$-$p)(\mu$-$CF_3C_2CF_3)$ (<4% yield). Spectroscopic data: IR (CH_2Cl_2) ν(CN) at 2125 s, ν(CO) at 1985 s cm^{-1}. In solution, this product converted rapidly to $(\eta$-$C_5H_5)_2Rh_2(CO)\{\mu$-$C(NC_6H_4OMe$-$p)C(CF_3)C(CF_3)\}$.

$(\eta$-$C_5H_5)_2Rh_2(CO)\{\mu$-$C(NC_6H_4NO_2$-$p)C(CF_3)C(CF_3)\}$ was the major product obtained from $(\eta$-$C_5H_5)_2Rh_2(\mu$-$CO)(\mu$-$CF_3C_2CF_3)$ and *p*-nitrophenyl isocyanide. It was isolated as an orange-brown solid (93% yield), mp 175 °C. Anal. Calcd for $C_{22}H_{14}F_6N_2O_3Rh_2$: C, 39.2; H, 2.1; F, 16.9; N, 4.2. Found: C, 40.4; H, 2.2; F, 17.2; N, 3.8. Spectroscopic data: IR (CH_2Cl_2) ν(CO) at 2005 vs and 1850 vs, ν(C=N) at 1680 vs and 1660 vs cm^{-1}; ^1H NMR ($CDCl_3$) δ 8.3–6.9 (several m, 4 H × 1.5, C_6H_4), 5.64 (br, 5 H × 1.44, C_5H_5 + C_5H_5'), 5.63 (s, 5 H × 0.06, C_5H_5''), 5.37 (d, 5 H × 0.06, C_5H_5''), 5.22 (br, 5 H × 1.44, C_5H_5 + C_5H_5'); ^{19}F NMR ($CDCl_3$) δ 52.4 (q, 3 F × 0.06, CF_3''), 52.9 (m, 3 F × 1.44, CF_3 + CF_3'), 52.2 (q, 3 F × 0.06, CF_3''), 56.2 (br, 3 F × 0.44, CF_3), 60.3 (br, 3 F, CF_3'); MS, m/z (relative intensity) 674 $[M]^+$ (<5), 646 $[M - CO]^+$ (18), 233 $[C_{10}H_{10}Rh]^+$ (100).

A minor product formed in the reaction was identified spectroscopically as $(\eta$-$C_5H_5)_2Rh_2(CO)(CNC_6H_4NO_2$-$p)(\mu$-$CF_3C_2CF_3)$. Spectroscopic data: ^1H NMR ($CDCl_3$) δ 8.28 and 7.31 (2 × d, 4 H, J = 9 Hz, C_6H_4), 5.49 (s, 10 H, 2 × C_5H_5); ^{19}F NMR ($CDCl_3$) δ 53.5 (s, CF_3).

Isomerization and Reaction Kinetics. Samples were prepared directly in sealed 5-mm NMR tubes by injecting a stoichiometric amount of the isocyanide into a solution of $(\eta$-$C_5H_5)_2Rh_2(\mu$-$CO)(\mu$-$CF_3C_2CF_3)$ in the appropriate solvent (1.0 mL). ^1H and ^{19}F NMR spectroscopy was used to monitor the reaction kinetics. Depending on the rate of isomerization, seven to eleven spectra were acquired over the reaction period. Integrals measuring peak areas corresponding to C_5H_5 or CF_3 groups were used to determine the relative quantities of the species present. Reaction rates were determined from a least-squares fit and the rate constants calculated by using the appropriate model[7] for the reaction. The errors quoted are one σ confidence limits. All calculations were performed by using a linear least-squares program on a "Dick Smith System 80" computer. Estimates of activation energies were made by using the formula $\Delta G^\ddagger = -RT \ln (k/k_BT)$ (k_B = Boltzman's constant, k = reaction rate).[7] Half-life estimates, $t_{1/2}$, were calculated by using the formula $t_{1/2} = \ln 2/k$ (k = reaction rate).

Crystallography. Crystals of $(\eta$-$C_5H_5)_2Rh_2(CO)\{\mu$-$C(NEt)C(CF_3)C(CF_3)\}$ were grown from dichloromethane/hexane. A representative crystal of dimensions (0.18 × 0.12 × 0.14 mm) was used for data collection. Intensity measurements were made on a Philips PW1100 computer controlled diffractometer with graphite-monochromated Mo Kα radiation (λ = 0.7107 Å) at 295 K. Cell parameters were determined from 24 accurately centered reflections and were calculated by the standard Philips program. Other crystal data are summarized in Table I. Three standard reflections monitored every 4 h showed no significant variation in intensity over the data collection period.

Intensity data were processed as described previously.[8] A numerical absorption correction was applied, the maximum and minimum transmission factors being 0.871 and 0.771, respectively. The atomic scattering factors for neutral atoms were taken from

(7) Schmid, R.; Sapunov, V. N. *Non-Formal Kinetics*; Verlag Chimie: Basel, 1982.

(8) Canty, A. J.; Chaichit, N.; Gatehouse, B. M. *Acta Crystallogr., Sect. B: Struct. Crystallogr. Cryst. Chem.* **1980**, *B36*, 786.

Table I. Summary of Crystal Structure Data for the Complex $(\eta\text{-}C_5H_5)_2Rh_2(CO)\{\mu\text{-}C(NEt)C(CF_3)C(CF_3)\}$

(a) Crystal Data	
formula	$C_{18}H_{15}F_6NORh_2$
mol wt	581.2
cryst system	monoclinic
space group	$P2_1/n$
a, Å	14.636 (8)
b, Å	11.277 (6)
c, Å	11.774 (6)
β, deg	92.86 (9)
U, Å^3	1940.9
Z	4
D(calcd), g cm^{-3}	1.99
D(measd), g cm^{-3}	2.00 (2)
F(000)	1128
μ(Mo Kα), cm^{-1}	15.9
(b) Data Collection	
2θ limits, deg	6–60
ω scan angle, deg	$\pm(0.75 + 0.20 \tan\theta)$
scan rate, deg s^{-1}	0.04
total data	5645
data $I > 3\sigma(I)$	2771
final R and R_w	0.056 and 0.056
weight w	$\sigma^{-2}(F)$

Table II. Final Positional Parameters for Complex 2, R = Et, $(\eta\text{-}C_5H_5)_2Rh_2(CO)\{\mu\text{-}C(NEt)C(CF_3)C(CF_3)\}$

atom	x	y	z
Rh(1)	0.21131 (5)	0.04636 (6)	−0.01115 (6)
Rh(2)	0.15563 (5)	0.25707 (6)	0.07093 (6)
F(1)	0.3934 (5)	0.3064 (7)	0.1445 (7)
F(2)	0.3293 (5)	0.1709 (7)	0.2363 (5)
F(3)	0.4275 (5)	0.1255 (7)	0.1189 (6)
F(4)	0.4558 (6)	0.2251 (10)	−0.0868 (11)
F(5)	0.4301 (6)	0.0508 (8)	−0.1059 (8)
F(6)	0.3864 (6)	0.1582 (13)	−0.2336 (7)
C(1)	0.1588 (7)	0.4547 (10)	0.0470 (9)
C(2)	0.0832 (8)	0.4242 (9)	0.1160 (9)
C(3)	0.0224 (7)	0.3550 (10)	0.0491 (9)
C(4)	0.0551 (7)	0.3410 (10)	−0.0609 (9)
C(5)	0.1445 (8)	0.4019 (9)	−0.0602 (9)
C(6)	0.2120 (10)	−0.1003 (12)	0.1188 (11)
C(7)	0.1264 (10)	−0.0838 (12)	0.0732 (11)
C(8)	0.1195 (11)	−0.1049 (13)	−0.0472 (12)
C(9)	0.2091 (9)	−0.1360 (11)	−0.0741 (10)
C(10)	0.2690 (9)	−0.1321 (12)	0.0300 (11)
C(11)	0.1436 (8)	0.1743 (10)	0.2019 (10)
C(12)	0.3583 (8)	0.1965 (11)	0.1351 (10)
C(13)	0.2837 (6)	0.1937 (8)	0.0422 (7)
C(14)	0.3022 (6)	0.1738 (8)	−0.0743 (7)
C(15)	0.3937 (9)	0.1528 (12)	−0.1255 (10)
C(16)	0.2209 (6)	0.1569 (8)	−0.1432 (7)
C(17)	0.1041 (9)	0.1292 (11)	−0.2868 (10)
C(18)	0.1221 (12)	0.0576 (15)	−0.3850 (14)
N	0.1887 (6)	0.1859 (8)	−0.2409 (7)
O	0.1335 (7)	0.1268 (8)	0.2879 (8)

ref 9 and were corrected for anomalous dispersion by using values from ref 9. All calculations were performed on a DEC/VAX 11/780 computer. The program used for least-squares refinement was that due to Sheldrick.[10] Hydrogen atoms were not included in the calculations.

The structure was solved by conventional Patterson and Fourier methods. In the full-matrix least-squares refinement, anisotropic temperature factors were employed for the Rh and F atoms; isotropic temperature factors were used for other atoms. Final positional parameters are given in Table II and selected interatomic distances and angles in Table III. Thermal parameters and some ligand geometries are deposited as supplementary material.

(9) Ibers, J. A., Hamilton, W. C., Eds. *International Tables for X-Ray Crystallography*; Kynoch: Birmingham, 1974; Vol. 4.
(10) Sheldrick, G. M. SHELX-76, Program for Crystal Structure Determination, Cambridge, England 1975.

Table III. Selected Bond Lengths and Angles for $(\eta\text{-}C_5H_5)_2Rh_2(CO)\{\mu\text{-}C(NEt)C(CF_3)C(CF_3)\}$

(a) Bond Distances (Å)			
Rh(1)–Rh(2)	2.706 (1)	C(12)–C(13)	1.51 (1)
Rh(1)–C(13)	2.052 (9)	C(13)–C(14)	1.43 (1)
Rh(1)–C(14)	2.118 (9)	C(14)–C(15)	1.51 (1)
Rh(1)–C(16)	2.003 (9)	C(14)–C(16)	1.42 (1)
Rh(2)–C(11)	1.819 (11)	C(16)–N	1.26 (1)
Rh(2)–C(13)	2.050 (9)	N–C(17)	1.47 (1)
C(11)–O	1.16 (1)	C(17)–C(18)	1.45 (2)
(b) Angles (deg)			
Rh(2)–Rh(1)–C(13)	48.7 (2)	Rh(1)–C(14)–C(13)	67.5 (5)
Rh(2)–Rh(1)–C(14)	74.7 (2)	Rh(1)–C(14)–C(15)	128.1 (8)
Rh(2)–Rh(1)–C(16)	76.4 (3)	Rh(1)–C(14)–C(16)	65.5 (5)
C(13)–Rh(1)–C(14)	40.1 (3)	C(13)–C(14)–C(15)	128.4 (9)
C(14)–Rh(1)–C(16)	40.2 (3)	C(13)–C(14)–C(16)	112.1 (8)
C(13)–Rh(1)–C(16)	71.3 (4)	C(15)–C(14)–C(16)	119.0 (8)
Rh(1)–Rh(2)–C(11)	84.0 (4)		
Rh(1)–Rh(2)–C(13)	48.8 (3)		
C(11)–Rh(2)–C(13)	95.1 (4)		
Rh(2)–C(11)–O	176.3 (11)	Rh(1)–C(16)–C(14)	74.3 (5)
		Rh(1)–C(16)–N	146.1 (8)
Rh(1)–C(13)–Rh(2)	82.6 (3)	C(14)–C(16)–N	138.5 (9)
Rh(1)–C(13)–C(14)	72.5 (5)		
C(12)–C(13)–Rh(1)	125.7 (7)	C(16)–N–C(17)	119.3 (9)
C(12)–C(13)–Rh(2)	120.6 (7)		
C(12)–C(13)–C(14)	122.3 (9)	N–C(17)–C(18)	110.7 (11)
C(14)–C(13)–Rh(2)	115.6 (6)		

Results

Formation of the complexes $(\eta\text{-}C_5H_5)_2Rh_2(CO)(CNR)(\mu\text{-}CF_3C_2CF_3)$ (**1**; R = Et, *i*-Pr, Cy, 2,6-$Me_2C_6H_3$) from $(\eta\text{-}C_5H_5)_2Rh_2(\mu\text{-}CO)(\mu\text{-}CF_3C_2CF_3)$ and the appropriate CNR has been described in a previous paper.[1] If left in solution, the complexes **1**, R = Et, *i*-Pr, or Cy but not 2,6-$Me_2C_6H_3$, isomerize to $(\eta\text{-}C_5H_5)_2Rh_2(CO)\{\mu\text{-}C(NR)C(CF_3)C(CF_3)\}$ (**2**). Similar reactions occur when CNR (R = Ph, *p*-$MeOC_6H_4$, *p*-$NO_2C_6H_4$) are added to $(\eta\text{-}C_5H_5)_2Rh_2(\mu\text{-}CO)(\mu\text{-}CF_3C_2CF_3)$. However, the isomerization reactions are so rapid with these systems that the initial addition products **1** cannot be isolated free of **2**. Nonetheless, the complexes **1** (R = Ph, *p*-$MeOC_6H_4$, *p*-$NO_2C_6H_4$) have been characterized spectroscopically in solution. Prolonged aging of the solutions containing **1** and **2** leads to some oxygenation of the products and the formation of bridging acrylamide complexes $(\eta\text{-}C_5H_5)_2Rh_2\{\mu\text{-}N(R)C(O)C(CF_3)C(CF_3)\}$ (**3**); complexes of this type have been characterized previously.[4] Substantial yields of the complexes **3** can be obtained by the deliberate oxygenation of **2** with trimethylamine *N*-oxide—these reactions are discussed in a previous paper.[1]

In all cases, the individual complexes **1**, **2**, and **3** can be separated by TLC of the reaction solutions. The chromatograms were not always well-defined, however, because there was streaking of the band due to **1**. If spectroscopically pure samples of **1** were dissolved in dichloromethane and immediately rechromatographed, streaking again occurred; this is attributed to enhancement by the chromatographic support of the rate of conversion of **1** to **2**. Although some isomerization of **2** to **1** occurred when spectroscopically pure samples of **2** were rechromatographed, only small amounts of **1** were formed; in one case (R = *p*-$MeOC_6H_4$), no *1* was evident. It thus seems that an equilibrium between **1** and **2** is established in solution and that it strongly favors **2**.

In the absence of the chromatographic support material, the isomerization of **1** to **2** is revealed by changes in the spectroscopic properties of solutions that are left to stand. For example, the infrared spectrum of a freshly prepared solution of **1**, R = *i*-Pr, in dichloromethane has $\nu(C{\equiv}N)$

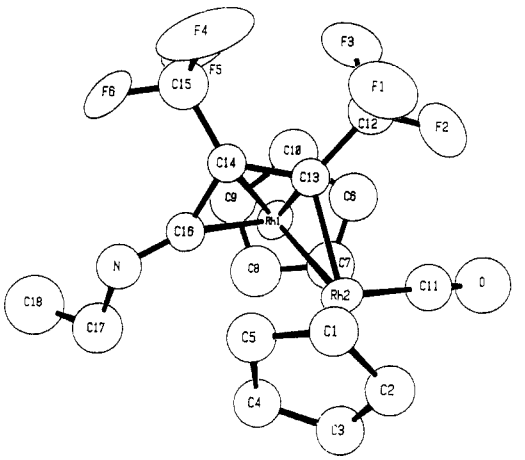

Figure 1. Molecular structure of the complex $(\eta\text{-}C_5H_5)_2Rh_2(CO)\{N(Et)C(CF_3)C(CF_3)\}$.

and $\nu(C{\equiv}O)$ absorption bands near 2150 and 2000 cm^{-1}, respectively, with approximate relative intensities of 8:10; no other bands are observed between 2000 and 1700 cm^{-1}. If the solution is left for about 7 days, the relative intensities of these bands change to approximately 3:10, and new bands appear near 1850 (relative intensity $\approx$ 3) and 1700 (relative intensity $\approx$ 5.5).

Similar changes are observed for complexes **1** with other R groups, and the rates of change are markedly dependent on the substituents R. It is very much faster for the aryl systems with R = Ph, p-$MeOC_6H_4$, or p-$NO_2C_6H_4$ but slower for the analogous CNCy system; no conversion is indicated when R = 2,6-$Me_2C_6H_3$, even when the solvent is refluxed. Since **1**, R = t-Bu, does not convert to the appropriate **2** in solution, it seems there is a steric barrier to the **1** $\rightarrow$ **2** conversion when R is large. For the other systems, the actual conversion rates have been determined from kinetic plots, and this is described later in this paper.

The IR spectra of pure samples of **2** are more complicated than would be expected for complexes of formula $(\eta\text{-}C_5H_5)_2Rh_2(CO)\{\mu\text{-}C(NR)C(CF_3)C(CF_3)\}$. In the solution phase, both terminal and bridging carbonyl groups are indicated by bands near 2040–2000 and 1890–1850 cm^{-1}, respectively. The spectra of solid samples of **2**, R = p-$MeOC_6H_4$ or p-$NO_2C_6H_4$, also show absorptions for both terminal and bridging carbonyls. However, the bridging carbonyl absorption is absent in the spectra of solid samples of **2**, R = Et, i-Pr, Cy, or Ph. These data indicate that **2** can exist in at least two isomeric forms. To determine the nature of the single isomer that crystallizes when solutions of the alkyl systems are evaporated, the crystal and molecular structure of the complex **2**, R = Et, was elucidated by X-ray crystallography.

Crystal and Molecular Structure of the Complex $(\eta\text{-}C_5H_5)_2Rh_2(CO)\{\mu\text{-}N(Et)C(CF_3)C(CF_3)\}$ (2, R = Et). The molecular structure is shown in Figure 1. It indicates that the CNR and $CF_3C_2CF_3$ groups have condensed with formation of a new C–C bond. The new ligand is best described as an allenimine, $\dot{C}(CF_3){=}{=}C(CF_3){=}{=}C{=}\dot{N}(Et)$; it is bound to a Rh–Rh single bond through the three allylic carbons. One terminal carbon, C(13), is equidistant from the two rhodium atoms (average Rh–C = 2.051 (9) Å). The other terminal carbon is attached to Rh(1) (Rh(1)–C(16) = 2.003 (9) Å), while the central carbon is also attached to Rh(1) (Rh(1)–C(14) = 2.118 (9) Å). The NEt group is bent away from the metals (C(14)–C(16)–N = 138.5°), and neither the imine (C=N) function nor the nitrogen lone pair is involved in bonding with the metal. All carbon atoms of the allylic system, including the two carbons of the CF_3 substituents, are coplanar,[11] and the dihedral angle between this plane and that defined by the non-hydrogen atoms of the NEt group is 30.0°. There is little difference between the two C–C distances in the allylic function. This is more consistent with the σ–π allylic bonding mode (**4a**) rather than the "vinyl–carbene" bonding mode (**4b**). The short C(16)–N distance (1.26 (1) Å) indicates double-bond character, which is consistent with the "imine" description. The coordination geometry around Rh(1) is completed by an η^5-attachment of a cyclopentadienyl group. An η^5-cyclopentadienyl group and a terminal carbonyl are attached to Rh(2).

Table IV. Summary of Spectroscopic Results for Selected Examples of 1 and the Isomers of 2

R	isomer	IR,[a] cm^{-1} ν(CO)	IR,[a] cm^{-1} ν(CN)	NMR[b] δ(Cp)	NMR[b] $\delta(CF_3)$
i-Pr	1	1990	2150	5.39	54.9
	2a	2000	1715, 1685	5.58, 5.29	52.1 qd, 55.8 q
	2b	1845		5.61	52.6 m, 60.1 m
	2c			5.55, 5.51	51.9 q, 54.8 q
p-$MeOC_6H_4$	1	1985	2125		
	2a	2005	1690, 1660	5.51, 5.29	52.7 q,[c] 55.6 br
	2b	1850			52.7 q,[c] 60.1 br
	2c				52.0 q, 54.9 q

[a] CH_2Cl_2 solution. [b] $CDCl_3$ solution. [c] Coincident peaks.

Scheme I

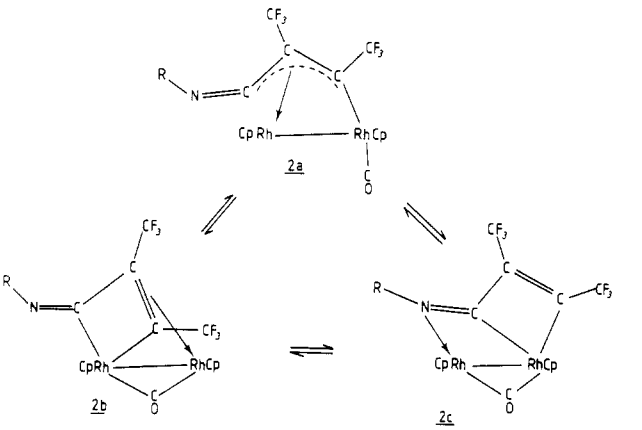

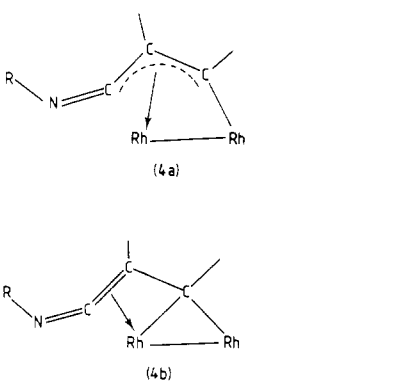

Solution Behavior of the Complexes 2. NMR Studies. The IR results discussed earlier indicate that at least two isomers of the complexes **2** coexist in solution. To gain more information about the solution behavior of these systems, some multinuclear NMR spectra were recorded. Results for two representative systems are summarized in Table IV, and they are interpreted in terms of

(11) Equations for the planes and deviations of atoms from the planes are presented as supplementary material.

three interconverting isomers in solution. Proposed structures for the isomers are shown in Scheme I. As shown below, the proportions and the rates of interconversion of the three isomers varies with the R group and the solvent.

^{19}F NMR. The ^{19}F spectra are easiest to interpret and will be considered first. Different characteristics are revealed in the spectra for alkyl (R = Et, *i*-Pr, Cy) and aryl (R = Ph, *p*-$MeOC_6H_4$, *p*-$NO_2C_6H_4$) systems, and consequently the two groups will be discussed separately.

The spectrum of the R = *i*-Pr complex is typical of the alkyl systems. In $CDCl_3$, six CF_3 resonances are observed and they can be divided into three pairs on the basis of the relative intensities and multiplicities (see Experimental Section). The peaks for the major isomer **2a** show the normal CF_3–CF_3 coupling with one peak showing additional coupling to Rh. For the minor isomers **2b** and **2c**, the resonances are observed as broad unresolved multiplets and quartets, respectively. Similar sets of resonances are detected in acetone-d_6 except that there is overlap of the low-field signals assigned to **2a** and **2c**. The ratio of **2a**:**2b**:**2c** is 13:1:1 in $CDCl_3$ but 5:1:1 in acetone-d_6. For the other alkyl systems, the corresponding ratios are 23:2:1 (R = Et; solvent = $CDCl_3$), 7:1:1 (Et; acetone-d_6), 11:1:1 (Cy; $CDCl_3$), and 6:1:1 (Cy; acetone-d_6).

The spectra of solutions of **2**, R = *i*-Pr, in acetone-d_6 have been measured over the temperature range +28 to −75 °C. The six CF_3 peaks are retained over the entire temperature range, but there are some changes in the overall profile of the spectrum. Some representative spectra and a tabulation of chemical shift changes with temperature are deposited as supplementary material. The various changes presumably reflect the effects of temperature on equilibria which relate the three isomers.

The spectra of **2**, R = *p*-$MeOC_6H_4$, are representative of the aryl systems. In $CDCl_3$, only five CF_3 signals are observed due to coincidence of one broad resonance for each of **2a** and **2b**. The spectrum in acetone-d_6 is similar, except that two broad peaks are observed for each of **2a** and **2b**. The proportion of the isomers is 20:8:1 in $CDCl_3$ but 5:3:1 in acetone-d_6. For the other aryl systems, the isomer ratios are 18:16:1 (R = Ph; solvent = $CDCl_3$), 3:5:1 (Ph; acetone-d_6), 7:16:1 (*p*-$NO_2C_6H_4$; $CDCl_3$), and 1:3:1 (*p*-$NO_2C_6H_4$; acetone-d_6). In contrast to the alkyl systems, **2b** is sometimes the predominant species in these systems.

The broadness of some of the peaks in these spectra prompted us to record the spectra of **2**, R = *p*-$MeOC_6H_4$, in acetone-d_6 over the temperature range +49 to −95 °C. Selected spectra are shown in Figure 2, and other data are deposited as supplementary material. Throughout the temperature range, the CF_3 resonances for **2c** remain as two well-defined quartets. Two CF_3 resonances are also expected for each of the isomers **2a** and **2b**, and both are observed at some temperatures. At −95 °C, the lower field resonance for **2a** overlaps the lower field resonance for **2b**, but the two resonances are clearly distinguished above ca. −76 °C. The fine structure of the peak for **2b** is lost above ca. −38 °C and that for **2a** above ca. −7 °C. Both peaks then broaden as the temperature is raised further, and they coalesce at 36 °C. The higher field resonances for each of **2a** and **2b** are well-separated at −95 °C. Again, these two peaks lose their fine structure and then broaden as the temperature is raised, and coalesence has almost been reached at 49 °C. These changes indicate that the equilibria between the isomers are established rapidly for **2a** and **2b**, but more slowly for **2c**. For solutions of **2**, R = *p*-$MeOC_6H_4$, in $CDCl_3$, coalescence of the two low-field signals for **2a** and **2b** is achieved at 25 °C, and this indicates that the rate of interconversion is faster in chloroform than in acetone. In chloroform, the temperature could be raised to 59 °C, but even then complete coalescence of the two higher field signals for **2a** and **2b** was not achieved.

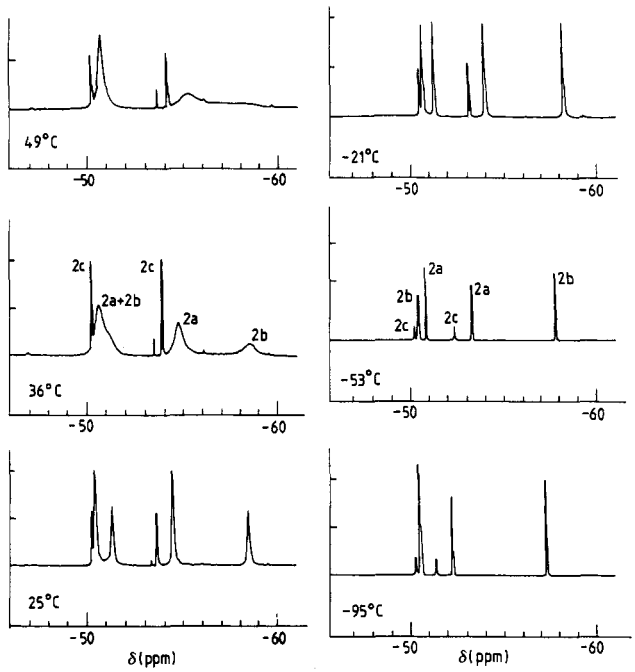

Figure 2. Comparison of the ^{19}F NMR spectra of the complex **2**, R = *p*-$MeOC_6H_4$, in acetone-d_6 at selected temperatures within the range +49 to −95 °C.

^{1}H NMR. A detailed examination of the corresponding ^{1}H spectra in the $\delta(C_5H_5)$ region provided support for the above ideas. Again, the appearance of the spectra is markedly different for the alkyl and aryl systems, and there is a solvent and a marked temperature dependence.

The spectrum of **2**, R = *i*-Pr, in acetone-d_6 at room temperature is dominated by two sharp C_5H_5 resonances that are assigned to **2a**. A cluster of small peaks is also evident, but assignments to the minor isomers **2b** and **2c** are not possible. At −76 °C, the two singlets for **2a** are still the most intense lines in the spectrum; these show no appreciable change as the solution is warmed. Another pair of singlets of much lower intensity are evident to low field of the other C_5H_5 signals. On the basis of relative intensities, these are assigned to **2c**. A single resonance at δ 5.82 presumably represents accidentally degenerate signals for the two C_5H_5 groups of the remaining isomer **2b**. As the temperature is raised, these three minor signals merge until only one signal is evident at −25 °C and above. Some representative spectra are deposited as supplementary material.

For the R = *p*-$MeOC_6H_4$ system (Figure 3), three sets of $(C_5H_5)_2$ signals are clearly evident at low temperature. In accord with the ^{19}F results, the most intense pair are assigned to **2a**, those of intermediate intensity to **2b**, and the lowest intensity pair to **2c**. The peaks due to **2a** and **2b** broaden as the temperature is raised, but those assigned to **2c** remain sharp. Eventually, there is coalescence of the lower field peak for **2a** with the lower field peak for **2b** and similarly of the two higher field peaks for the two isomers. Coalescence is achieved at ca. 5 °C, and the coalescence peaks continue to sharpen as the temperature is raised to and above room temperature. Although these peaks are still somewhat broad in acetone at 49 °C, sharp singlets are seen in chloroform at 59 °C.

^{13}C NMR. A limited amount of supporting data can be extracted from the ^{13}C NMR spectra of ^{13}CO-enriched

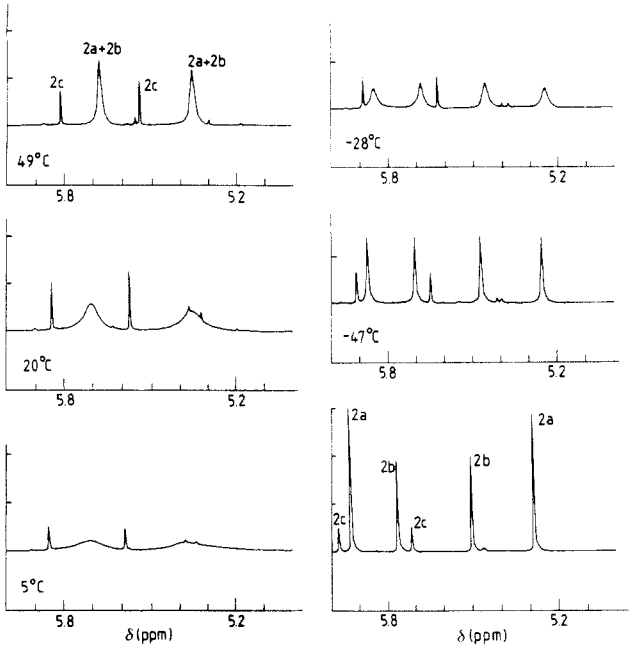

Figure 3. Comparison of the ^1H NMR spectra of the complex **2**, R = *p*-$MeOC_6H_4$, in acetone-d_6 at selected temperatures within the range +49 to −95 °C.

samples of **2**, R = *i*-Pr or *p*-$MeOC_6H_4$. For the *p*-$MeOC_6H_4$ system in $CDCl_3$ at −38 °C, two carbonyl resonances are clearly seen. One is observed as a doublet of doublets at δ 212, and this is assigned to the bridging carbonyl of **2b**. The terminal carbonyl of **2a** is found as a doublet at δ 189. Unfortunately, no carbonyl signal is observed for **2c**; this is not surprising given the low proportion of this isomer indicated in the ^{19}F and ^1H spectra. As the temperature of the solution is raised to 0 and then 28 °C, the carbonyl signals broaden significantly. This is consistent with an increased rate of interconversion between **2a** and **2b**. The remainder of the ^{13}C spectrum can also be analyzed in terms of the coexistence of the isomers **2a** and **2b**.

As expected, the spectrum of the *i*-Pr system is dominated by peaks attributed to **2a**. The terminal carbonyl peak at δ 189 is observed as a doublet of doublets with couplings to the two rhodium nuclei of 82 and 4 Hz. There is an additional terminal carbonyl peak at δ 191. This is a relatively weak doublet at 25 °C but becomes a more intense triplet when the temperature of the solution is raised to 57 °C. This behavior is typical[12,13] of that of a terminal carbonyl which can scramble rapidly from one rhodium to the other when the temperature is raised. This peak is attributed to the presence of some **1** in the solution; presumably, the long accumulation times enable an equilibrium between **2** and **1** to be established. No signals for **2b** or **2c** could be recognized in the spectrum.

Kinetics for the Interconversion Reaction Involving 1, 2a, 2b, and 2c. The rates of isomerization of **1** to the three isomers of **2** have been determined from analysis of changes in the ^1H (C_5H_5 region) and ^{19}F NMR spectra with time. Generally, RNC was added to a solution of $(\eta\text{-}C_5H_5)_2Rh_2(\mu\text{-}CO)(\mu\text{-}CF_3C_2CF_3)$, the initial formation of **1** was witnessed, and the subsequent formation of **2** was followed in situ. It was assumed that **1** directly rearranges to all three isomers of **2**, and this was validated for those systems where significant amounts of all isomers are formed. The isomers **2a**, **2b**, and **2c** are formed at the same time since the rate of appearance of each of the isomers is equivalent to the rate of disappearance of **1**. The species **2a**, **2b**, and **2c** then interconvert with each other and establish equilibria which are dependent on the substituent on the isocyanide and the solvent. The reactions were generally followed for up to about 6 half-lives provided no significant decomposition was evident before this time had elapsed. The kinetic model fitted to each reaction was based on those described by Schmid and Sapunov[7] for simple first-order reactions. Three different types of kinetic behavior were recognized, and a representative example of each class is discussed below. The model used to define each system is described in supplementary material.

Table V. Kinetic and Thermodynamic Data for Isomerization Reactions 1 → 2 at 297 K (k in $s^{-1} \times 10^{-5}$; $t_{1/2}$ in min)

	R/solvent		
system[a]	*i*-Pr/$CDCl_3$	Ph/acetone-d_6	*p*-$NO_2C_6H_4$/acetone-d_6
1 → 2			
k	1.3 ± 0.4	32 ± 4	420 ± 20
$\Delta G^{\ddagger}$[b]	+101	+93	+86
1 ⇌ 2a			
k_{1+}	1.2 ± 0.5	75 ± 17	1300 ± 300
$t_{1/2}$	990 ± 410	15 ± 4	0.9 ± 0.2
k_{1-}	0.12 ± 0.05	26 ± 6	irreversible
$t_{1/2}$	9950 ± 4140	46 ± 11	
K	10	2.9	
1 ⇌ 2b			
k_{2+}	not determined	51 ± 12	460 ± 90
$t_{1/2}$	23 ± 5	2.5 ± 0.5	
k_{2-}	9.4 ± 2.2	irreversible	
$t_{1/2}$	120 ± 29		
K	1.1	5.5	
1 ⇌ 2c			
k_{3+}	not determined	120 ± 30	1700 ± 300
$t_{1/2}$	9.5 ± 2.4	0.7 ± 0.1	
k_{3-}	75 ± 17	irreversible	
$t_{1/2}$	15 ± 4		
K	0.97	1.6	
2a ⇌ 2b			
K	0.088		2.4
2a ⇌ 2c			
K	0.080		0.79
2b ⇌ 2c			
K	0.91	3.1	

[a] For the system *i*-Pr/$CDCl_3$, **2** = **2a**; for Ph/acetone-d_6 and *p*-$NO_2C_6H_4$/acetone-d_6, **2** = **2a** + **2b** + **2c** and **2** = **2a** + **2b**, respectively. [b] kJ mol^{-1}; the error for $\Delta G^{\ddagger}$ is almost negligible and is approximaaed from $(\Delta G^{\ddagger}_{max} - \Delta G)$ where $\Delta G^{\ddagger}_{max}$ is calculated from $(k + k_{error})$.

The CN-*i*-Pr system in $CDCl_3$ is formulated as a reversible first-order reaction:

$$1 \underset{k_{1-}}{\overset{k_{1+}}{\rightleftharpoons}} 2a \qquad (1)$$

Kinetic and thermodynamic data (see Table V) indicate that isomerization to **2a** is strongly favored but that the rate is relatively slow; the rate of the reverse reaction is exceedingly slow. Although the concentrations of **2b** and **2c** are low in these systems, it is possible to approximate the equilibrium constants for interconversion reactions involving these species by using the approximate mole fractions and assuming equilibrium is established after about 6 half-lives. Similar behavior is found for the system with R = Cy and solvent = $CDCl_3$, and results are provided as supplementary material.

For the aryl system with R = Ph, the kinetic behavior in acetone-d_6 is interpreted in terms of three reversible, first-order, parallel reactions (eq 2). The data in Table

(12) Dickson, R. S.; Mok, C.; Pain, G. N. *J. Organomet. Chem.* **1979**, *166*, 385.
(13) Dickson, R. S.; Oppenheim, A. P.; Pain, G. N. *J. Organomet. Chem.* **1982**, *224*, 377.

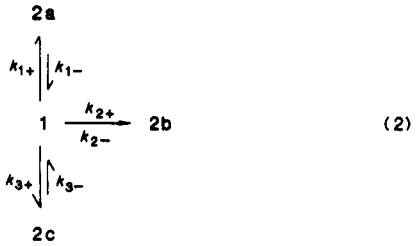

(2)

V reveal several interesting differences from the alkyl systems. The rates are much higher for the aryl system, the equilibrium constant for the formation of **2a**, R = Ph, is lower but that for **2b**, R = Ph, formation is significantly higher. Similar data has been obtained for the system R = *p*-$MeOC_6H_4$ in $CDCl_3$ and is available as supplementary material.

For the system with R = *p*-$NO_2C_6H_4$ and solvent = acetone-d_6 the conversion is best formulated as three parallel, nonreversible, first-order reactions The indi-

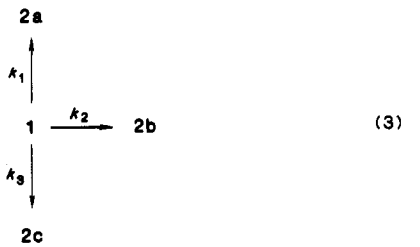

(3)

vidual rate constants (Table V) are large in comparison to the alkyl and other aryl systems, and these values correspond to very short half-lives. The data is consistent with no reverse reaction (**2a** + **2b** + **2c**) → **1**, but an equilibrium mixture of the three isomers of **2** is still obtained. Presumably they interconvert according to

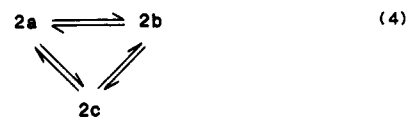

(4)

Approximate equilibrium constants for these steps have been determined. Limited data was also obtained for the *p*-$NO_2C_6H_4$ system in $CDCl_3$. The rate of isomerization in this solvent is twice that in acetone-d_6.

Discussion

A Rationalization of the Solution Behavior of 2 and the Characterization of 2a–c. For all alkyl systems, the major isomer **2a** is almost certainly the one that can be crystallized from solution. This has been fully characterized from X-ray diffraction data for the compound with R = Et. The ligand arrangement is shown in Scheme I, and the IR and NMR results are consistent with retention of this structure in solution. In some aryl systems, the corresponding isomer **2a** seems to crystallize together with a second major isomer **2b**.

The ease of interconversion between **2a** and the other isomers suggests there are no major structural changes upon isomerization. A reasonable structure for **2b** is shown in Scheme I. It is consistent with the observed spectroscopic properties (Table IV) and is analogous to that established[14] for $(\eta\text{-}C_5Me_5)_2Rh_2(\mu\text{-}CO)\{\mu\text{-}C(O)C(CF_3)C(CF_3)\}$ except that an imine replaces the acyl group in the metallocyclic system. The CF_3 quartets in the spectra of **2b** show $J_{FF} \approx 7$ Hz. This coupling constant is about half that usually found in complexes with the *cis*-$C(CF_3)C(CF_3)$ unit

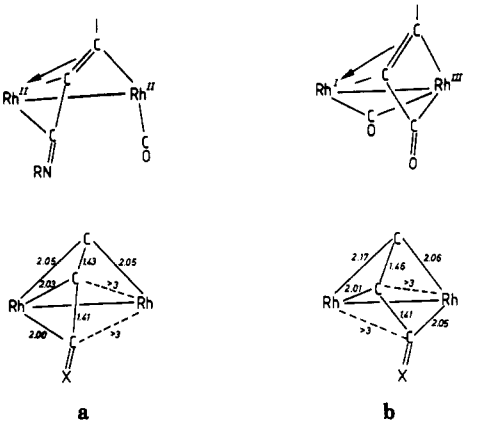

a b

Figure 4. Comparison of selected bond length data for the complexes (a) $(\eta\text{-}C_5H_5)_2Rh_2(CO)\{N(Et)C(CF_3)C(CF_3)\}$ (**2a**) and (b) $(\eta\text{-}C_5Me_5)_2Rh_2(\mu\text{-}CO)\{C(O)C(CF_3)C(CF_3)\}$. For clarity the cyclopentadienyl rings are omitted from all diagrams and the carbonyl ligands from the bottom two.

but is identical with that found in $(\eta\text{-}C_5Me_5)_2Rh_2(\mu\text{-}CO)\{\mu\text{-}C(O)C(CF_3)C(CF_3)\}$; this provides strong support for the proposed structure. Figure 4 compares the structural features of **2a**, R = Et, with those of $(\eta\text{-}C_5Me_5)_2Rh_2(\mu\text{-}CO)\{\mu\text{-}C(O)C(CF_3)C(CF_3)\}$ which is used as a model for **2b**. It is clear that only minor movements of the ligand atoms are needed to achieve the isomerization **2a** → **2b**.

A possible structure for **2c** is more difficult to elucidate. The IR results indicate that **2c** probably incorporates bridging CO and imine C=NR groups, and the NMR data show inequivalence of the two C_5H_5 and the two CF_3 groups. A reasonable structure is shown in Scheme I, and it is derived by small movements of the atoms in either **2a** or **2b**. The imine-substituted metallacyclobutene ring in this proposed structure (and in that suggested for **2b**) is similar to the ring system which has been structurally characterized[15] for some $(\eta\text{-}C_5H_5)Co(PR_3)\{C(NR')C(R)C(R)\}$ complexes. In Scheme I, coordination from the lone pair on the imine nitrogen is indicated. However, it is conceivable that an η^2-C=N coordination to the second Rh atom operates instead; such a coordination mode is established,[16] for example, in the complex $(\eta\text{-}C_5H_5)Mo(CO)_2(\eta^2\text{-}CMe{=}NPh)$. Consideration of the three structures included in Scheme I reveals some interesting changes in the formal oxidation states of the two metal atoms. These are I and II in **2a**, III and I in **2b**, and I and III in **2c**.

In attempting to rationalize the effects of R on the rate and extent of the isomerization reactions, it is necessary to consider both steric and electronic effects. The bulk of R can clearly be important since there is no isomerization at all when R = *t*-Bu or 2,6-$Me_2C_6H_3$. With the systems studied kinetically, however, steric factors seem relatively unimportant. The observed order of rates of isomerization of **1** to **2**, and of interconversions between the isomers of **2**, is Cy < *i*-Pr < Ph < *p*-$MeOC_6H_4$ < *p*-$NO_2C_6H_4$. This approximately parallels the expected electronic effects[17] of these substituents, the one exception being the relative positions of Ph and *p*-$MeOC_6H_4$. This minor discrepancy, plus the major difference in the observed rates for alkyl and aryl systems, indicates that additional effects associated with the aromatic rings are significant. It appears that any para substituent, electron withdrawing (NO_2) or electron donating (MeO), assists the

(14) Dickson, R. S.; Evans, G. S.; Fallon, G. D. *Aust. J. Chem.* **1985**, *38*, 273.

(15) Wakatsuki, Y.; Miya, S.-Y.; Ikuta, S.; Yamazaki, H. *J. Chem. Soc., Chem. Commun.* **1985**, 35.

(16) Adams, R. D.; Chodosh, D. F. *Inorg. Chem.* **1978**, *17*, 41.

(17) Tolman, C. A. *Chem. Rev.* **1977**, *77*, 315.

conversion reaction, presumably by affecting the charge density at the reaction site. Estimates of the free energies of activation for the 1 → 2 isomerization are included in Table V, and the values for the alkyl systems are considerably higher than those of the aryl complexes. This reinforces the idea that electronic factors are important in determining the activation energy and hence the rate of the isomerization reactions.

Oxygenation of Complexes 2. When solutions of the complexes **2** are left exposed to the air, there is a slow conversion of **2** to the bridging acrylamide complexes **3**. A better way to achieve this conversion is through the deliberate oxygenation of **2** with Me_3NO in refluxing acetone.[1] When R is an aryl substituent, conversions of 50–90% are achieved within a few hours; smaller amounts of **3** are obtained with the alkyl systems. Since CO_2 is evolved in these reactions, there is oxygen transfer from Me_3NO to both CO and the imine carbon in **2**. It is known[18] that terminal carbonyls are most susceptible to attack by Me_3NO, and therefore **2a** is probably the reactive species in solution.

Summary and Conclusions

This study of the $\{(\eta\text{-}C_5H_5)_2Rh_2(\mu\text{-}CO)(\mu\text{-}CF_3C_2CF_3)$ + CNR$\}$ system demonstrates that a single alkyne and isocyanide ligands can condense on a binuclear metal center to form a coordinated allenimine. The new ligands can adopt a number of coordination modes, and three are represented in the isomers revealed by NMR analysis of solutions of the product. The rates of formation of the allenimine complex and of interconversions between the isomeric forms are markedly dependent on the isocyanide substituent R. Rates are faster when R is an aryl group and slower for the alkyl systems. Electronic factors account for the rate differences, but steric factors can completely inhibit the reactions when R is very bulky.

Acknowledgment. We are grateful to the Australian Research Grants Scheme (R.S.D.) for financial support of this project and to Johnson-Matthey for the loan of hydrated rhodium trichloride. H.P. thanks the Commonwealth Government for a Postgraduate Research Award.

Registry No. **1** (R = Et), 110294-86-5; **1** (R = *i*-Pr), 98464-05-2; **1** (R = Cy), 98464-04-1; **1** (R = Ph), 110488-33-0; **1** (R = *p*-$MeOC_6H_4$), 110488-37-4; **1** (R = *p*-$NO_2C_6H_4$), 110488-41-0; **2a** (R = Et), 110488-21-6; **2a** (R = *i*-Pr), 110488-24-9; **2a** (R = Cy, 110488-27-2; **2a** (R = Ph), 110488-30-7; **2a** (R = *p*-$MeOC_6H_4$), 110488-34-1; **2a** (R = *p*-$NO_2C_6H_4$), 110488-38-5; **2b** (R = Et), 110488-22-7; **2b** (R = *i*-Pr), 110488-25-0; **2b** (R = Cy), 110488-28-3; **2b** (R = Ph), 110488-31-8; **2b** (R = *p*-$MeOC_6H_4$), 110488-35-2; **2b** (R = *p*-$NO_2C_6H_4$), 110488-39-6; **2c** (R = Et), 110488-23-8; **2i** (R = *i*-Pr), 110488-26-1; **2c** (R = Cy), 110488-29-4; **2c** (R = Ph), 110488-32-9; **2c** (R = *p*-$MeOC_6H_4$), 110488-36-3; **2c** (R = *p*-$NO_2C_6H_4$), 110488-40-9; $(\eta\text{-}C_5H_5)_2Rh_2(CO)(CF_3C_2CF_3)$, 98395-25-6; CNPh, 931-54-4; CNC_6H_4OMe-*p*, 10349-38-9; $CNC_6H_4NO_2$-*p*, 1984-23-2.

Supplementary Material Available: Tables of thermal parameters, ligand geometries, and equations for planes for $(\eta\text{-}C_5H_5)_2Rh_2(CO)\{\mu\text{-}C(NEt)C(CF_3)C(CF_3)\}$ and tables and figures of spectroscopic and kinetic data for $((\eta\text{-}C_5H_5)_2Rh_2(CO)\{\mu\text{-}C(NR)C(CF_3)C(CF_3)\}$ complexes (22 pages); a listing of structure factor amplitudes for $(\eta\text{-}C_5H_5)_2Rh_2(CO)\{\mu\text{-}C(NEt)C(CF_3)C(CF_3)\}$ (16 pages). Ordering information is given on any current masthead page.

(18) Luh, T.-Y. *Coord. Chem. Rev.* **1984**, *60*, 255.

Synthesis and Molecular Structure of Chlorobis(tetraphenylcyclopentadienyl)titanium(III). Synthesis and Variable-Temperature ^1H NMR Study of Dichlorobis(tetraphenylcyclopentadienyl)titanium(IV)

Michael P. Castellani,[1a] Steven J. Geib,[1b] Arnold L. Rheingold,*[1b] and William C. Trogler*[1a]

Department of Chemistry, D-006, University of California at San Diego, La Jolla, California 92093, and Department of Chemistry, University of Delaware, Newark, Delaware 19716

Received April 2, 1987

The reaction between either $TiCl_2$ or $TiCl_3$ and $K(C_5HPh_4)$ yields $(C_5HPh_4)_2TiCl$ (I). A green crystal of $(C_5HPh_4)_2TiCl\cdot CH_2Cl_2\cdot(C_4HO)_{1/2}$ obtained on recrystallization belongs to the triclinic space group $P\bar{1}$ with a = 12.878 (4) Å, b = 14.586 (5) Å, c = 15.888 (4) Å, α = 63.08 (2)°, β = 79.10 (2)°, γ = 63.67 (2)°, Z = 2, and V = 2385 Å^3. The molecular structure, determined by refinement on 4281 reflections greater than or equal to $4\sigma(F_o)$, converged to R_F = 6.13% and R_{wF} = 6.05%. The complex crystallizes as well-separated monomeric units with the tetraphenylcyclopentadienyl rings staggered to form an inter-ring centroid angle of 136.4° and a short Ti–Cl bond length of 2.312 (2) Å. The Ti–C bond lengths vary by 0.155 Å, and the phenyl groups bend away from Ti because of steric congestion at the metal. Solution EPR studies show evidence for free $(C_5HPh_4)_2TiCl$ (g = 1.957) and for a THF adduct (g = 1.979). Oxidation of I with AgCl cleanly produces $(C_5HPh_4)_2TiCl_2$ (II), which can be isolated. Dynamic ^1H NMR studies of II show evidence for restricted rotation of the phenyl substituents with $\Delta G^{\ddagger}$ = 9.6–10.0 kcal/mol. Reduction of a THF solution of I with sodium naphthalide under argon produces an unstable brown mixture; however, addition of CO yields a species with IR absorptions at 1966 and 1892 cm^{-1}, which suggests the formation of $(C_5HPh_4)_2Ti(CO)_2$.

Introduction

Previous work on octaphenylmetallocenes has shown that the sterically bulky tetraphenylcyclopentadienyl ligand greatly reduces the reactivity of these complexes, as compared to the unsubstituted metallocenes.[2] Solid-state and solution structural studies have permitted an under-

(1) (a) University of California at San Diego. (b) University of Delaware.

(2) Castellani, M. P.; Geib, S. J.; Rheingold, A. L.; Trogler, W. C. *Organometallics* **1987**, *6*, 1703.

0276-7333/87/2306-2524$01.50/0 © 1987 American Chemical Society